Zitierweise: *Angew. Chem. Int. Ed.* **2020**, *59*, 17413–17416
Internationale Ausgabe: doi.org/10.1002/anie.202005425
Deutsche Ausgabe: doi.org/10.1002/ange.202005425

Porphyrinoids

Stereoselective On-Surface Cyclodehydrofluorization of a Tetraphenylporphyrin and Homochiral Self-Assembly

Hui Chen[+], Lei Tao[+], Dongfei Wang, Zhuo-Yan Wu, Jun-Long Zhang, Song Gao, Wende Xiao, Shixuan Du, Karl-Heinz Ernst,* and Hong-Jun Gao**

Abstract: *The thermally induced cyclodehydrofluorization of iron tetrakis(pentafluorophenyl)porphyrin proceeded highly stereoselectively to give a prochiral product on a gold surface in an ultrahigh vacuum, whereas dehydrocyclization of the respective iron tetrakisphenylporphyrin did not show such selectivity. Stereoselectivity was predominantly observed for closely packed layers, which is an indication of intermolecular cooperativity and steric constraints induced by adjacent species. Density functional theory identified intermolecular packing constraints as the origin of such selectivity during the reaction. Scanning tunneling microscopy revealed the formation of an enantiomerically pure two-dimensional self-assembly as a conglomerate of mirror domains. On-surface two-dimensional topochemistry, as reported herein, may open new routes for stereoselective synthesis.*

In 1919 Volkmar Kohlschütter reported for certain solid-state reactions that the product of a chemical reaction may rely on the relative arrangement of reactants fixed in space and termed it "topochemistry".[1] In particular the pioneering work of Gerhard Schmidt on solid-state photochemistry revealed then the profound stereoselectivity of reactions in the crystalline state.[2] In general, topochemistry is characterized by relative reactant alignment due to confinement and should therefore play an important role in two-dimensional (2D) systems, such as molecular monolayers on solid surfaces, where the adsorbates are surface-aligned prior to reaction.

It has been shown for helicenes in thermally induced decomposition or C–C coupling reactions that reactant alignment due to selective interaction with a surface induces stereoselectivity.[3–5] Moreover, the lateral interaction between reactants and thus their relative alignment in the plane has an influence on the reaction pathway.[6] An example related to stereoselectivity is heterogeneously catalyzed enantioselective hydrogenation of α- and β-keto esters to chiral alcohols, in which the prochiral reactant becomes aligned enantiotopically by a chiral modifier on the surface.[7] However, only few surface chemistry studies report an influence of 2D density (i.e., coverage) on the outcome of the reaction. For example, a higher yield of metalation of porphyrins by partially lifting the macrocycle above the surface due to increased lateral interactions at higher coverage has been reported.[8]

Scanning tunneling microscopy (STM) shows that iron(II) tetrakis(pentafluorophenyl)porphyrin ($FeF_{20}TPP$, **1**, Scheme 1) undergoes a quadruplicate intramolecular cyclization on the Au(111) surface upon thermal treatment. Due to the possibility of dehydrofluorization at either side of the F_5C_6 group, formation of four isomers should be expected. However, basically one windmill-like product is observed with pronounced excess after cyclization (Scheme 1). The prochiral planar product subsequently self-assembles into densely packed enantiopure mirror domains upon cooling. At high surface coverages and sufficient heating rates the stereose-

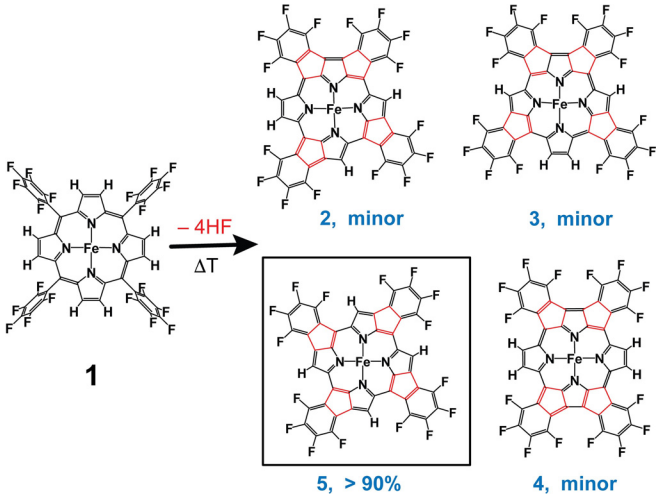

Scheme 1. On-surface intramolecular quadruple ring formation after cyclodehydrofluorization of $FeF_{20}TPP$. Four different porphyrins with different symmetries were produced. The reaction proceeded highly stereoselectively to give prochiral product **5** in over 90% yield.

[*] Dr. H. Chen,[+] Dr. L. Tao,[+] Dr. D. Wang, Prof. Dr. W. Xiao, Prof. Dr. S. Du, Prof. Dr. H.-J. Gao
Institute of Physics and University of Chinese Academy of Science
Chinese Academy of Science
Beijing 100190 (P. R. China)
E-mail: sxdu@iphy.ac.cn
hjgao@iphy.ac.cn
Dr. Z.-Y. Wu, Prof. Dr. J.-L. Zhang, Prof. Dr. S. Gao
Beijing National Laboratory for Molecular Sciences, State Key Laboratory of Rare Earth Materials Chemistry and Applications
College of Chemistry and Molecular Engineering, Peking University
Beijing 10087 (P. R. China)
Prof. Dr. K.-H. Ernst
Empa
Swiss Federal Laboratories for Materials Science and Technology
Überlandstrasse 129, 8600 Dübendorf (Switzerland)
E-mail: karl-heinz.ernst@empa.ch
[+] These authors contributed equally to this work.
Supporting information and the ORCID identification number(s) for the author(s) of this article can be found under: https://doi.org/10.1002/anie.202005425.

lective yield can be as high as 90%. By means of density functional theory (DFT) it is shown that such stereoselectivity has its origin in the intermolecular steric constraints in the self-assembled structure of **1** on Au(111) prior to reaction.

All STM experiments were performed at 5 K with electrochemically etched tungsten tips and were calibrated against the electronic surface state of the Au(111) surface before and after tunneling spectroscopy measurements. The Au(111) surface was prepared by repeated cycles of sputtering with argon ions and annealing at 800 K. FeF_{20}TPP molecules were prepared from FeF_{20}TPP-Cl deposited onto the Au(111) surface held at room temperature and subsequent annealing to 400 K (see Supporting Information), which leads to desorption of chlorine, leaving the metal porphyrin intact on the surface (Figure S1).[9]

Adsorbed on Au(111), FeF_{20}TPP exhibits a saddle-shape conformation which is a characteristic feature of metal porphyrins adsorbed on metal surfaces.[10] The molecules self-assemble into ordered close-packed structures with a rectangular unit cell containing two molecules with different azimuthal orientation (Figure 1a). The difference between the molecular azimuthal angles is $120 \pm 1°$, reflecting the Au(111) surface symmetry (Figure 1b). The unit cell parameters are $a = 1.47 \pm 0.02$ nm, $b = 2.89 \pm 0.01$ nm and $\alpha = 91 \pm 2°$.

After thermal annealing to 600 K, the FeF_{20}TPP molecules were converted into planar product, also self-assembling into a new 2D structure on the Au(111) surface (Figure 1c). The unit cell (indicated by the white square box in Figure 1c) of the newly formed structure is: $a = b = 1.71 \pm 0.01$ nm and $\alpha = 90 \pm 1°$. High-resolution STM images show that the planar product exhibits C_4 symmetry, which is only consistent with product **5**. Confined to a surface, such product becomes chiral.[11] Two coexisting types of mirror domains, marked as δ and λ in Figure 1c, are observed in STM images. The enantiomorphous nature of the self-assembly is manifested in respective counterclockwise and clockwise alignments of the molecules in the domains (Figure 1d,e).

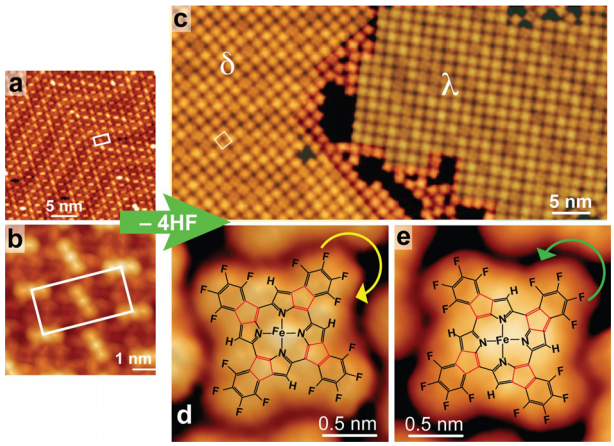

Figure 1. STM images of molecular layer before and after annealing. a) STM image of **1** self-assembled on Au(111). b) STM image as in (a) but at larger magnification. The two molecules in the unit cell are rotated by 120° to each other. c) STM image after heating the sample to 550 K, showing two adjacent mirror domains (δ, λ). d,e) High-resolution STM images of single product molecules taken from the mirror domains. The superposition of product **5** agrees best. Windmill-like configurations of opposite handedness (indicated by circular arrows) are identified. (STM parameters: a,c: $U = -0.1$ V, $I = 0.01$ nA; b,d,e: $U = -0.2$ V, $I = 0.1$ nA; all STM images taken at 5 K).

All ordered domains exclusively contained product **5** while products **2**, **3**, **4** were only observed in small disordered patches at the domain boundaries (Figure S2). The relative yield of product **5** is higher than 90%, indicating the high regioselectivity in **1** of the reaction. A similar selectivity in cyclodehydrogenation has been only observed for 2H-tetraphenylporphyrin (TPP) due to its twofold symmetry but not for the fourfold-symmetric metalated TPP.[12] At lower coverages, however, the stereoselectivity towards product **5** is less pronounced. Figures 2a–c show STM images of the final products, starting at coverages of 0.1 ML, 0.3 ML and 0.9 ML of **1**, respectively. The achieved yield of product **5** for these experiments scales clearly with the initial coverages (Figure 2d). Such observation points to an intermolecular cooperative effect, meaning that close-packing favors the stereoselectivity.

Besides coverage, the heating rate is also crucial for the selectivity towards product **5**. At lower heating rates the selectivity drops significantly, even for high-coverage samples. The STM images of three samples after heating to 600 K are shown in Figure 2e–g. In terms of uniformity the best sample containing **5** as building block is achieved at a heating rate of 15 K min^{-1}, highlighted also by the statistical area analysis shown in Figure 2h. Such observation suggests that reaction kinetics is likewise crucial for the selectivity. It is known that faster heating leads to higher desorption temperatures in temperature-programmed desorption experiments.[13] But desorption of HF is here not the rate-limiting step, because it leaves immediately after formation. However, if the reaction temperature shifts to higher temperatures as for desorption with higher heating rate, the reaction rate will be substantially higher, and any competing temperature-induced rearrangement will have a smaller influence during time of reaction.

In stepwise annealing experiments (i.e. 540 K, 560 K, 580 K and 600 K) self-assembly of intermediates which underwent partially cyclization was also studied. All expected intermediate species were identified in STM at incomplete reaction stage, when a semi-ordered self-assembly still occurred (Figure S3 and S4).

DFT calculations were performed on single intermediates and products on a 3-layer Au(111) substrate slab (see Supporting Information S5 for details). Although reaction barriers should be evaluated, the universality principle in the Brønsted–Evans–Polanyi relation for surface reactions allows correlation of the adsorption energy to the activation energy,[14] in particular because dehydrofluorization and C–C bond formation of each step are very similar here. Therefore, the calculated ground-state energies of possible intermediates on Au(111) can be used to evaluate the reaction pathway (Supporting Information S6). The total energies of product **2**, **3**, **4** are 0.26 eV, 0.24 eV and 0.56 eV higher than that of product **5**, which means product **5** is more favorable. This seems already an indication that product **5** is the most

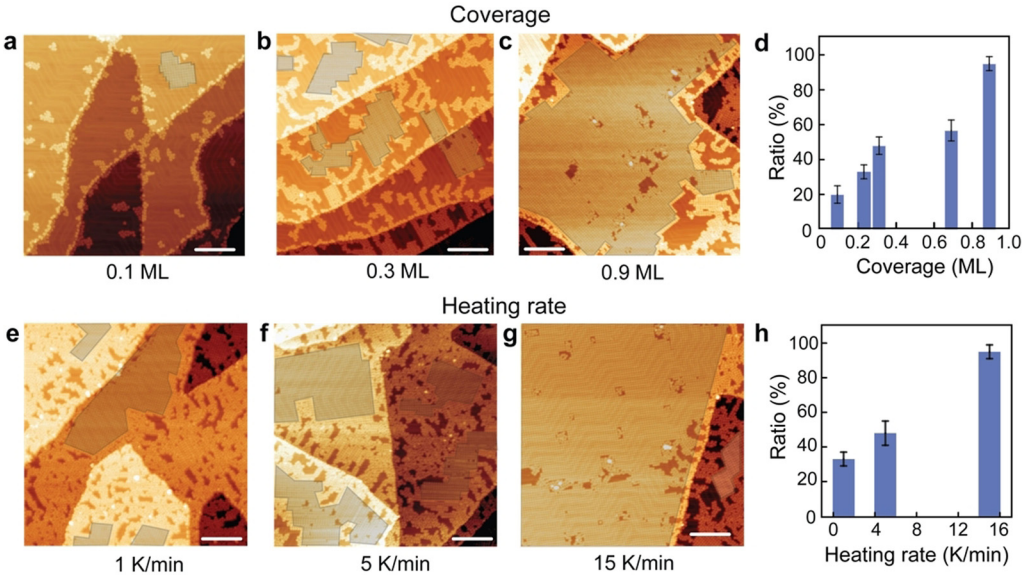

Figure 2. Effects of coverage and heating rates on the regioselectivity of ring-fusion reactions. a–c) STM images of the reaction-induced self-assembly for different initial coverages of **1** ($U = -0.6$ V, $I = 0.05$ nA) at a heating rate of 15 K min^{-1}. d) Histogram of area covered with **5** versus initial coverage of **1**. e–g) STM images of the reaction-induced self-assembly after heating at different rates ($U = -0.6$ V, $I = 0.05$ nA, 0.9 ML of **1**). h) Histogram of areal density of **5** versus heating rate during annealing. ML = monolayer.

favorable. However, a statistical analysis of the four products observed in STM images of disordered areas shows that product **2** is the most favorable, which disagrees with the expected ratio based on the DFT calculations. But it does not show significant deviations from the expected frequencies based solely on probability (see Supporting Information S2).

In order to simulate the coverage dependence of the observed stereoselectivity and to support the qualitative scenario of steric constraints due to close-packing, the following model has been used for further

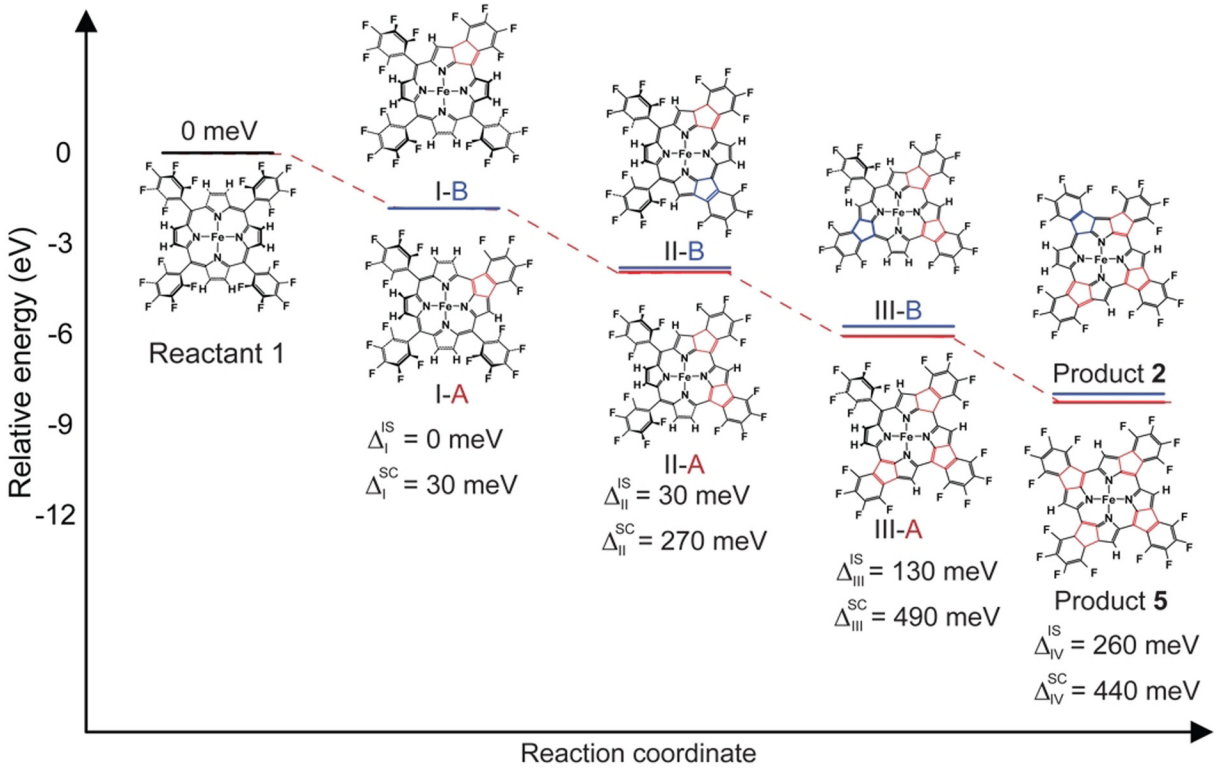

Figure 3. Structural and energetic evolution from reactant **1** to products **2** and **5** on Au(111). There are three intermediates, I, II, and III, in each pathway. A and B represent the intermediates along the reaction pathway for product **5** and **2**, respectively. Configurations shown are the reactant and the intermediates and final products which have the lowest (I-A, II-A, III-A, and **5**) and second lowest energies (I-B, II-B, III-B, and **2**) in each step. Δ_I^{IS}, Δ_{II}^{IS}, Δ_{III}^{IS}, and Δ_{IV}^{IS} are energy differences between the two structures when there is an isolated intermediate, whereas Δ_I^{SC}, Δ_{II}^{SC}, Δ_{III}^{SC}, and Δ_{IV}^{SC} are the energy differences considering steric constraints originating from the adjacent molecules. The eight relaxed final configurations, including surface and surrounding reactant molecules, are presented in Figure S7 of the Supporting Information.

DFT calculations. As for isolated molecules, ground-state adsorption energies are believed to correlate with activation barriers and were calculated for all intermediates considering steric constraints during the reaction pathway. Therefore, the two product species **2** and **5** as well as their intermediates are placed and relaxed in a fixed matrix of six reactants (Supporting Information S7). The central species and the differences in energies are summarized in Figure 3. There is no notable difference in the first step, but all following steps favor the path to the observed final product. The difference between the statistically favored species **2** and the observed final product **5** amounts to 0.44 eV. Especially in combination, the energetics of the reaction steps will strongly favor product **5**. Hence, the calculations support the experimental observations.

In summary, the thermally induced intramolecular cyclization reactions of $FeF_{20}TPP$ on Au(111) at monolayer saturation coverage proceeds with high stereoselectivity into a prochiral product, that self-assembles into a 2D conglomerate of enantiopure domains. DFT calculations performed on model structures of intermediates and products imbedded in a matrix of reactants confirm that the origin of stereoselectivity originates from intermolecular steric constraint imposed during reaction. It is anticipated that topochemistry based on surface-confined systems, as demonstrated here for the intramolecular cyclodehydrofluorization, can be exploited for stereochemical control.

Acknowledgements

We thank Prof. Sokrates T. Pantelides for helpful discussions. We acknowledge financial support from the National Key Research & Development Projects of China (2016YFA0202300), the National Natural Science Foundation of China (No. 61888102), Strategic Priority Research Program of the Chinese Academy of Sciences (Grant No. XDB30000000), K. C. Wong Education Foundation. Part of the work was performed in CAS Key Laboratory of Vacuum Physics. The calculations have been performed at the National Supercomputer Center in Tianjin. K.-H.E. gratefully acknowledges support provided by the European Union for a Mobility Professorship, the Sino Swiss Science and Technology Cooperation (SSSTC) for travel subsidies, and the Swiss National Science Foundation for continuous support.

Conflict of interest

The authors declare no conflict of interest.

Keywords: chirality · fluorine · on-surface chemistry · porphyrinoids · topochemistry

[1] V. Kohlschütter, *Z. Anorg. Allg. Chem.* **1919**, *105*, 1 – 25.
[2] M. D. Cohen, G. M. J. Schmidt, *J. Chem. Soc.* **1964**, *383*, 1996 – 2000.
[3] O. Stetsovych, M. Švec, J. Vacek, J. V. Chocholoušová, A. Jančařík, J. Rybáček, K. Kosmider, I. G. Stará, P. Jelínek, I. Starý, *Nat. Chem.* **2017**, *9*, 213 – 218.
[4] A. Mairena, C. Wäckerlin, M. Wienke, K. Grenader, A. Terfort, K.-H. Ernst, *J. Am. Chem. Soc.* **2018**, *140*, 15186 – 15189.
[5] C. Wäckerlin, J. Li, A. Mairena, K. Martin, N. Avarvari, K.-H. Ernst, *Chem. Commun.* **2016**, *52*, 12694 – 12697.
[6] Q. Chen, J. R. Cramer, J. Liu, X. Jin, P. Liao, X. Shao, K. V. Gothelf, K. Wu, *Angew. Chem. Int. Ed.* **2017**, *56*, 5026 – 5030; *Angew. Chem.* **2017**, *129*, 5108 – 5112.
[7] H.-U. Blaser, *Tetrahedron: Asymmetry* **1991**, *2*, 843 – 866.
[8] a) M. Röckert, S. Ditze, M. Stark, J. Xiao, H.-P. Steinrück, H. Marbach, O. Lytken, *J. Phys. Chem. C* **2014**, *118*, 1661 – 1667; b) M. Röckert, M. Franke, Q. Tariq, S. Ditze, M. Stark, P. Uffinger, D. Wechsler, U. Singh, J. Xiao, H. Marbach, H. P. Steinrück, O. Lytken, *Chem. Eur. J.* **2014**, *115*, 8948 – 8953.
[9] a) B. W. Heinrich, G. Ahmadi, V. L. Müller, L. Braun, J. I. Pascual, K. J. Franke, *Nano Lett.* **2013**, *13*, 4840 – 4843; b) J. M. Gottfried, *Surf. Sci. Rep.* **2015**, *70*, 259 – 379; c) M. Turner, O. P. Vaughan, G. Kyriakou, D. J. Watson, L. J. Scherer, G. J. Davidson, J. K. Sanders, R. M. Lambert, *J. Am. Chem. Soc.* **2009**, *131*, 1910 – 1914; d) M. Turner, O. P. Vaughan, G. Kyriakou, D. J. Watson, L. J. Scherer, A. C. Papageorgiou, J. K. Sanders, R. M. Lambert, *J. Am. Chem. Soc.* **2009**, *131*, 14913 – 14919.
[10] W. Auwärter, D. Ecija, F. Klappenberger, J. V. Barth, *Nat. Chem.* **2015**, *7*, 105 – 120.
[11] K.-H. Ernst, *Surf. Sci.* **2013**, *613*, 1 – 5.
[12] A. Wiengarten, J. A. Lloyd, K. Seufert, J. Reichert, W. Auwärter, R. Han, D. A. Duncan, F. Allegretti, S. Fischer, S. C. Oh, Ö. Sağlam, L. Jiang, S. Vijayaraghavan, D. Écija, A. C. Papageorgiou, J. V. Barth, *Chem. Eur. J.* **2015**, *21*, 12285 – 12290.
[13] P. A. Redhead, *Vacuum* **1962**, *12*, 203 – 211.
[14] a) J. K. Nørskov, T. Bligaard, A. Logadottir, S. Bahn, L. B. Hansen, M. Bollinger, H. Bengaard, B. Hammer, Z. Sljivancanin, M. Mavrikakis, Y. Xu, S. Dahl, C. J. H. Jacobsen, *J. Catal.* **2002**, *209*, 275 – 278; b) F. A. Carey, R. J. Sundberg, *Advanced Organic Chemistry (Part A: Structure and Mechanisms)*, 5th ed., Springer, New York, **2007**.

Manuscript received: April 14, 2020
Accepted manuscript online: June 30, 2020
Version of record online: August 11, 2020

